A thermal camera survey trial of the wild horse population in Kosciuszko National Park, NSW, October–November 2024

Report to the NSW Department of Climate Change, Energy, the Environment & Water, February 2025

[redacted]

Abstract

1. In 2024 the NSW National Parks and Wildlife Service asked us to do an aerial survey of horses in four priority management areas in Kosciuszko National Park (KNP), to estimate the 2024 horse populations using the same methods used in recent years. Alongside standard survey methodology using aerial observers, they also requested a trial of high-definition thermal cameras during the same flights, for comparison. Surveys were conducted in October–November 2024.

2. Results of the human aerial observer survey have been reported on separately. This report gives results of the thermal survey using two Vayu high-definition cameras. Where relevant comparisons with results of the human-observer aerial survey are made.

3. More than 2,000 km of transect line was flown for the 2024 survey. Flying height and aircraft speed were the same as in the October 2023 survey. Flight times were kept within 3 hours of sunrise and sunset. Surveys were done in a Park Air Eurocopter (B3 Squirrel) helicopter with the doors off. Two thermal cameras, fitted with 25 mm (32.1° vertical field of view) lenses, recorded footage at 60 frames/second. They were pointed perpendicular to the aircraft's track, and were angled down 40° from the horizon. This provided a ~110-m strip width (swathe) on the ground on both sides of the aircraft.

4. After the survey, thermal camera footage was reviewed by human observers. Horses and foals were counted by pausing the footage and clicking on individual animals as they appeared in the frame. Observers also recorded habitat structure (open/medium/dense) for horse sightings. All data collection was reviewed by a second observer. Data was exported and analysed using multiple covariate distance sampling (MCDS).

5. No horses were sighted on the thermal imagery in the Cabramurra Block, so it was excluded from the analysis. Data were analysed for the Northern, Southern, and Snowy Plains survey blocks. Data was first analysed for the entire dataset combined, and then stratified for each survey block separately.

6. MCDS modelling identified temperature as the covariate with greatest effect on adult horse detectability. Using the best model, population density was 1.070 adult horses/ km^2. When horses + foals were combined, the best model showed temperature and camera position (left or right) had most influence on detections. This model gave a density of 1.116 horses + foals/km^2.

7. The stratified analyses gave similar population/abundance estimates for the Northern and Southern survey blocks (**Adult horses:** Northern, 1,369; Southern 1,226. **Horses + foals:** Northern 1,293; Southern 1,420). As expected, the much smaller Southern Plains block had a much smaller population (151 adult horses, or 164 horses + foals).

8. Thermal cameras gave similar estimates to the human observers for the Snowy Plains, but there is insufficient data for this small block for a meaningful comparison. Human observer estimates were higher than thermal camera estimates for the Northern Block. Conversely, in the Southern Block, thermal camera estimates were higher than the human observer MCDS estimates, and approached the MRDS estimates when adult

horses + foals were included. Overall, thermal camera estimates were lower than MRDS estimates in all blocks.

9. The thermal cameras missed some horses that human observers saw, likely due to horses flushing away from the helicopter before they entered the narrower field of view of the camera. Random sampling of 130 groups of horses seen by human observers showed that the thermal cameras missed 50% of those seen by aerial observers in the furthest sighting zones. This could theoretically be countered by angling the cameras forward, but this would violate the mathematical assumptions of distance sampling.
10. If flushing behaviour is the main reason for lower horse detections by cameras, helicopters are probably unsuitable for thermal surveys of horses. Quieter electric drones may be more appropriate.

This report may be cited as:

[redacted] (2025). A thermal camera survey trial of the wild horse population in Kosciuszko National Park, NSW, October–November 2024. *Report to the NSW Department of Climate Change, Energy, the Environment & Water, February 2025.*

Version & revision history	Authors	Reviewed by	Date
Version 1 – 14/02/2025	[redacted]		
Version 2 – 19/03/2025 (included additional analysis of effects of flushing behaviour on the thermal camera results)	[redacted]	NSW National Parks & Wildlife Service	09/05/2025
Version 3 – 30/05/2025	[redacted]	[redacted]	30/06/2025
Version 4 – 03/07/2025	[redacted]		

[redacted]

DISCLAIMER

This report was prepared by [redacted] in good faith, exercising all due care and attention, but no representation or warranty, express or implied, is made as to the relevance, accuracy, completeness or fitness for purpose of this document in respect of any particular user's circumstances. Users of this document should satisfy themselves concerning its application to, and where necessary seek expert advice in respect of, their situation. The views expressed within are not necessarily the views of the Department of Climate Change, Energy, the Environment and Water and may not represent department policy.

Introduction

Background

The Australian Alps National Parks (AANP) network, in the Great Dividing Range of eastern Australia, straddles parts of New South Wales (NSW), Victoria, and the Australian Capital Territory (ACT). The AANP comprises a number of discrete parks spread across these three jurisdictions. The largest of these is Kosciuszko National Park (KNP), which is sited wholly within NSW, and has an area of 689,000 ha (6,890 km^2). It is managed by National Parks and Wildlife Service (NPWS) NSW.

Wild horses (*Equus caballus*) occupy various parts of KNP. Periodic population monitoring is necessary to manage the size and distribution of the horse population in line with the Kosciuszko National Park Wild Horse Heritage Management Plan (Environment & Heritage Group, 2021; amended 2023).

Aerial surveys are often the most cost-effective method of estimating the distribution, density and abundance of medium to large mammals over wide geographical areas. In previous aerial surveys of the KNP, horses have been counted by trained aerial observers. In 2024 this method was used alongside a second counting method for comparison. High-resolution thermal cameras, which have previously been used in aerial surveys of other medium- to large vertebrates species and in other regions, were mounted on both sides of the aircraft and recorded footage during all flights. Horses were later counted in the thermal camera footage by trained observers, providing a dataset that was used to estimate horse population density and abundance in the KNP. The purpose of this thermal camera aerial survey trial was to compare the performance of this method relative to the results obtained from the human observer counts.

Consistent with previous surveys of KNP, the human-observer population density and abundance estimates for 2024 were derived using the commonly-used techniques of Conventional Distance Sampling (CDS) and Multiple-Covariate Distance Sampling (MCDS). An additional method, Mark-recapture Distance Sampling (MRDS), which typically uses data from three observers rather than the usual two (Thomas *et al.* 2006), was also added in 2024 (see [redacted] 2024a). MRDS analyses and corrects for the proportion of animals missed by the observers, and generally results in upward revision of the population density estimate. Data from the thermal camera counts was analysed using MCDS. Consistent with the aerial-observer data, separate population density estimates were calculated for adult horses only, and adult horses plus foals. These results are presented below, and are compared with the results from the simultaneous aerial-observer survey (see [redacted] 2024a).

Methods

Study area

As described in [redacted] (2024a), four survey blocks of the KNP Wild Horse Heritage Management Areas have previously been identified by NPWS NSW as key areas

that support populations of wild horses: the Northern, Snowy Plains, Cabramurra, and Southern survey blocks (see Figure 1). The Northern (1,229 km^2) and Southern (1,146 km^2) blocks are an order of magnitude larger than the Snowy Plains (161 km^2) and Cabramurra (139 km^2) blocks.

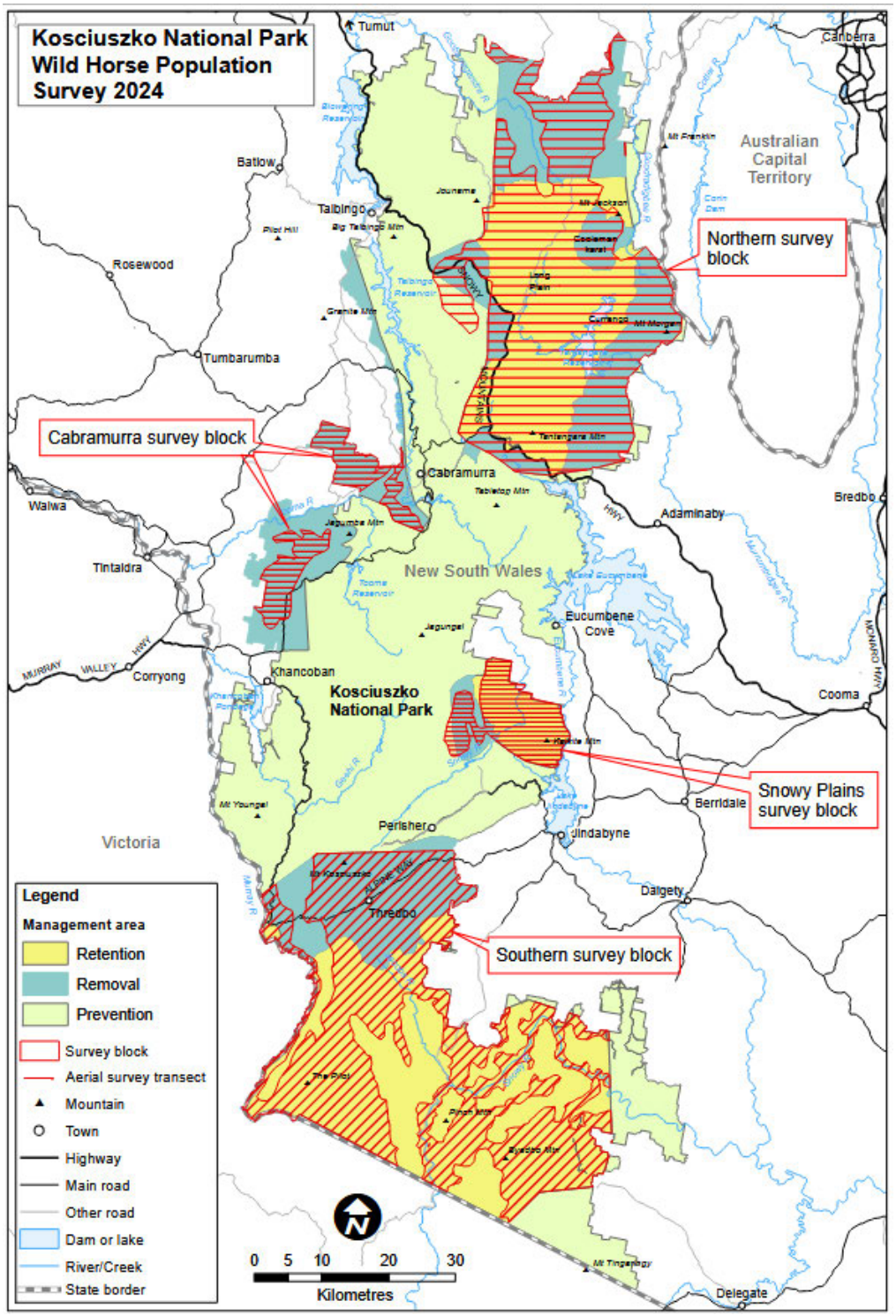

Figure 1: *Map of the Kosciuszko National Park Wild Horse Heritage Management Areas, showing the four management areas surveyed for this report. The aerial transect lines flown in 2024 are shown in red. Map supplied by NSW National Parks & Wildlife Service.*

Survey design

The 2024 survey was designed to follow a similar format to [redacted] (2020; 2022; 2023), with amendments to the amount of survey effort in some of the blocks based on analysis of previous years' survey data (see [redacted] 2024a). Parallel transect lines were flown in each survey block, avoiding areas with steep topography (see Figure 1).

Flying operations

Aerial survey work was conducted between 27th October and 10th November 2024 using a Park Air Eurocopter (B3 Squirrel) single-engine helicopter with the rear doors open to improve sightability. Ground speed was held at 93 km/h (50 kts) at a height of 61 m (200 ft) above ground level. The pilot used a GPS receiver to keep on track.

To ensure surveys coincided with the times of day when horses were thought to be most active, all flights were scheduled to be completed within 3 hours of first light and last light. Surveying was avoided when weather conditions would negatively affect visibility of animals or it was deemed unsafe to fly by the pilot.

Thermal cameras

Two uncooled microbolometer Sierra Olympia Vayu HD (1,200 x 1,900 pixel) thermal cameras (Sierra-Olympia Technologies Inc. 2020) were mounted on fixed mounts on either side of the aircraft, behind the front seats, and captured video frames at a rate of 60 frames per second. The cameras were pointed perpendicular to the aircraft's track and maintained a 40° dip from the horizon. A 25 mm (32.1° vertical field of view) lens was fitted to each, which provided ~110-m full strip width (swathe) on the ground at 200 feet AGL, on both sides of the aircraft. This dip from the horizon is optimised so that the effective viewing area (the Effective Strip Width, or ESW; see definition on p.9) on each side of the aircraft is less than 100 m. Previous experience shows that a shallower angle (less than 40° from the horizon) leads to excessive pixelation of animals further away from the aircraft, leading to a decline in sightability/identifiability, while missing animals closer to the aircraft that would have been identifiable. At an angle of 40° down from the horizon, any decline in sightability with greater distance is likely due to factors other than pixelation, e.g. reduced sightability due to obstruction by vegetation, which can then be modelled using MCDS.

Thermal footage processing & animal counts

All thermal camera footage was processed using Program *Thermal* (Lethbridge 2019) to help detect hotspots. Because the aircraft and camera are in a constant forward motion, some noise is apparent in a horizontal direction, sometimes requiring an anisotropic (directional) de-speckling algorithm to be anisotropic. When this is required the algorithm de-speckles stationary static noise in the imagery. Following the above corrections, an adaptive thresholding AI algorithm can then be applied if necessary. Moreover, an AI learning algorithm is employed. This is taught to recognise hotspots identified by human desktop observers.

After the conclusion of the aerial survey, observers viewed the processed thermal camera footage in *Thermal*, using large-format computer screens with high-end graphics cards to maximise image clarity. Observers searched the footage and identified the species presented. Each mammal seen in the footage was classified manually (e.g. horse, foal, deer, kangaroo, unknown), along with habitat density where the animal was sighted (open, medium, dense). For species where we have previous AI training data that automatically recognises hotspots likely to be animals, hotspots are usually highlighted in the camera footage before being classified by a human observer, as a guide only. However, as we had no previous AI learning data on horses, observers instead viewed the thermal imagery exhaustively to allow the AI algorithms to learn the detections for future surveys, if required.

After the first pass, for additional data quality control, a second experienced aerial observer checked the first observer's classifications independently; any misclassifications were corrected. Only human observers with aerial survey experience made the final decision about the classification of each hotspot in the video footage.

For each flight video, the outputs from the desktop observer's classifications were stored in a proprietary file format, which records the species, habitat density classification, pixel location (*x,y*), and video frame number of each animal sighting.

These desktop data were then processed by Program *FrameLinkMulti* Version 1.0 (Lethbridge 2022), which combines multiple video frames for each flight, synchronised with aircraft GPS track data recorded by Program *RGIS* (Lethbridge 2018) in the air. At 60 frames per second, the time is tagged to the video frames rather than GPS coordinates because this frame rate is too fast for GPS frame tagging.

For each animal identified in the thermal footage, the software calculates its equivalent perpendicular ground distance in metres, converted from pixel coordinate out from the bottom of each camera frame and a known flying height. This basic trigonometry also enables the calculation of real-world coordinates for each animal. A single output file of all animals, stratified by transect and survey block is then imported into Program *Distance* 8 (Thomas *et al.* 2010) to model population density.

Multiple Covariate Distance Sampling

Multiple Covariate Distance Sampling (MCDS; Buckland *et al*. 1993) was used to process the thermal imagery data in Program *Distance* 8 (Thomas *et al.* 2010). MCDS allowed us to test the influence that various combinations of covariates could have had on detectability of animals in the thermal camera footage. Covariates tested in the model were sun direction, temperature, humidity, the time to/since darkness, camera position (left or right) and vegetation density. Extreme temperatures and humidity were tested because they are thought to affect camera performance. Propeller wash can affect camera image quality and given there are differences in the strength of propeller wash between the left and right side of this aircraft, the position of the camera was tested as a covariate. Temperature and humidity readings were taken from the BoM Thredbo weather station, recorded at 3 p.m. and 9 a.m. each day, with some missing readings at this gauge supplemented by readings from nearby Cooma station. Helicopter temperature and humidity readings were not used

because these are always confounded by aircraft height above the ground (colder) and propellor wash.

MCDS takes into account the decay in the probability of seeing an animal with an increasing distance from the aircraft. It uses a detection function $g(x)$, which is the probability of detecting an object at distance x, the perpendicular distance out from the aircraft. It is assumed that $0.0 \leq g(x) \leq 1.0$. The equivalent probability density function fitted through a frequency histogram of observations is denoted $f(x)$.

The final density equation for one side of a transect line is given by Equation 1.

$$\hat{D} = \frac{n}{Lw\hat{P}} \qquad \textbf{Equation 1}$$

Here $\hat{D}$ is the density being estimated, n is the observed counts, L is the length of the sample area, w is the total width of the sample area, and $\hat{P}$ is the overall probability that a randomly located object in the sample area is in fact detected (Buckland *et al.* 1993). This only accounts for perception bias. The product of $\hat{P}$ and w is also known as the Effective Strip Width (ESW). ESW is the area under $g(x)$ curve outward from $x = 0$. This statistically derived metric is the effective perpendicular distance that the cameras see out from the aircraft. It is the distance at which the same fraction of animals is missed inside the ESW as observed beyond.

Akaike's Information Criterion (AIC; Akaike 1974) was used to rank all the covariate models within the model set from 'best' to 'worst' relative to each other. The lowest AIC score indicates the best-fitting model for the fewest parameters (known as model parsimony). The coefficient of variation (CV), another indicator of a good model fit, was also calculated.

In the camera footage, and distinct from survey data collected by aerial observers, the location of each individual animal is recorded, rather than groups of animals. Analyses of the effects of group size are therefore not relevant to the thermal data.

Results

No horses were sighted on the thermal imagery in the Cabramurra Block during the 2024 surveys. As a consequence this block has been left out of population density modelling. The results presented below relate to the remaining three blocks only.

Multiple covariate distance sampling (MCDS)

Adult horses only

MCDS model outputs are shown in Table 1, ranked from best (lowest AIC score; in bold) to worst. In addition to sightability decay (the only factor tested in conventional distance sampling), the MCDS models assessed the effects of habitat (open, medium or dense), sun

direction, camera position in the aircraft, the closest time (in decimal hours) to either first light or last light, temperature and humidity.

The best-performing MCDS model (bold in Table 1) showed that adult horse detection was marginally affected by colder temperature. This model had an ESW of 62.0 m, and estimated an overall average adult horse population density of 1.070 horses per km^2 across all the included survey blocks combined (Table 1).

A histogram showing the decay in sightability with increasing distance from the aircraft (using the top-ranked model from Table 1) is plotted in Figure 2. While an alternative Hazard Rate model was tested, the line of best fit through the data used a Half-normal Cosine adjusted model (see red line in Figure 2). This shows that the sightability of adult horses due to pixelation, decayed gradually, from a probability of around 1.0 at the base of the camera frame to just over 0.2 at a distance of 100 m (equivalent ground distance) out from the frame's base.

As temperature was identified as the only covariate in the global model (Table 1), the effects of temperature on sightability are shown in Figure 3 under three scenarios (5°, 15°, and 23°C). It should be noted that above approximately 23°C, thermal imagery is known to degrade rapidly because the ground and tree trunks heat up, leading to insufficient contrast with animal heat signatures, and as a result we did not fly in these temperatures. Very cold temperatures are considered to have a much smaller effect on thermal image detections, and thus was tested as a covariate in this project, rather than ceasing flying operations. Weather station data was used as a proxy for temperature conditions during the survey, and it should be noted that these report temperatures at 9 a.m. or 3 p.m., and therefore might not accurately reflect temperature at the time the survey transects were flown. The temperatures recorded at the Thredbo weather station while we flew ranged from 3 to 23°C.

Table 1: *Multiple covariate distance sampling (MCDS) models tested for adult horse density estimates in three survey blocks of Kosciuszko National Park, 2024 (Cabramurra block was excluded due to insufficient data). The most parsimonious model (lowest AIC score) is shown in bold.* ***Abbreviations:*** *AIC – Akaike's Information Criterion; ESW – effective strip width (m); D – density (horses per km^2); D LCL – density lower 95% confidence limit; D UCL – density upper 95% confidence limit; CV – coefficient of variation. All models are a half-normal model.*

Model	Delta AIC	AIC	ESW	D	D LCL	D UCL	D CV
Temp	**0.0**	**2473.5**	**62.0**	**1.070**	**0.738**	**1.553**	**19%**
Temp (Strata)	0.0	2473.5	62.0	1.070	0.736	1.556	19%
Temp + Cloud + Camera	0.0	2473.5	61.7	1.075	0.740	1.561	19%
Temp + Cloud	0.2	2473.7	61.8	1.074	0.740	1.558	19%
Temp + Humidity+ Sun	1.9	2475.4	61.5	1.078	0.743	1.566	19%
Habitat + Temp	1.9	2475.4	61.8	1.073	0.739	1.557	19%
Temp + Humidity	2.0	2475.5	61.9	1.072	0.739	1.555	19%
Temp + Humidity + Cloud	2.1	2475.6	61.7	1.075	0.741	1.561	19%
Temp + Humidity+ Sun + Camera	2.3	2475.9	61.6	1.077	0.742	1.564	19%
Habitat + Temp + Humidity + Sun	3.6	2477.2	61.6	1.076	0.741	1.562	19%
Habitat + Temp + Humidity	3.9	2477.5	61.9	1.071	0.738	1.554	19%
Habitat + Temp + Humidity + Cloud	4.1	2477.6	61.8	1.074	0.740	1.558	19%
Habitat	13.0	2486.5	63.3	1.047	0.723	1.518	19%
Habitat + Cloud	13.2	2486.7	63.1	1.052	0.726	1.524	19%
Habitat + Humidity	13.7	2487.2	63.1	1.050	0.725	1.523	19%
Habitat + Humidity + Sun	14.0	2487.5	63.0	1.053	0.726	1.526	19%
Habitat + Sun	14.0	2487.5	63.2	1.049	0.724	1.520	19%
Habitat + HTD	15.0	2488.5	63.3	1.047	0.723	1.518	19%
Habitat + Sun + HTD	15.9	2489.4	63.3	1.048	0.723	1.519	19%
DEFAULT_HORSE	23.9	2497.4	65.5	1.013	0.694	1.480	19%
Sun	25.7	2499.2	65.4	1.014	0.700	1.468	19%
Cloud + Sun	26.1	2499.7	65.4	1.014	0.700	1.469	19%

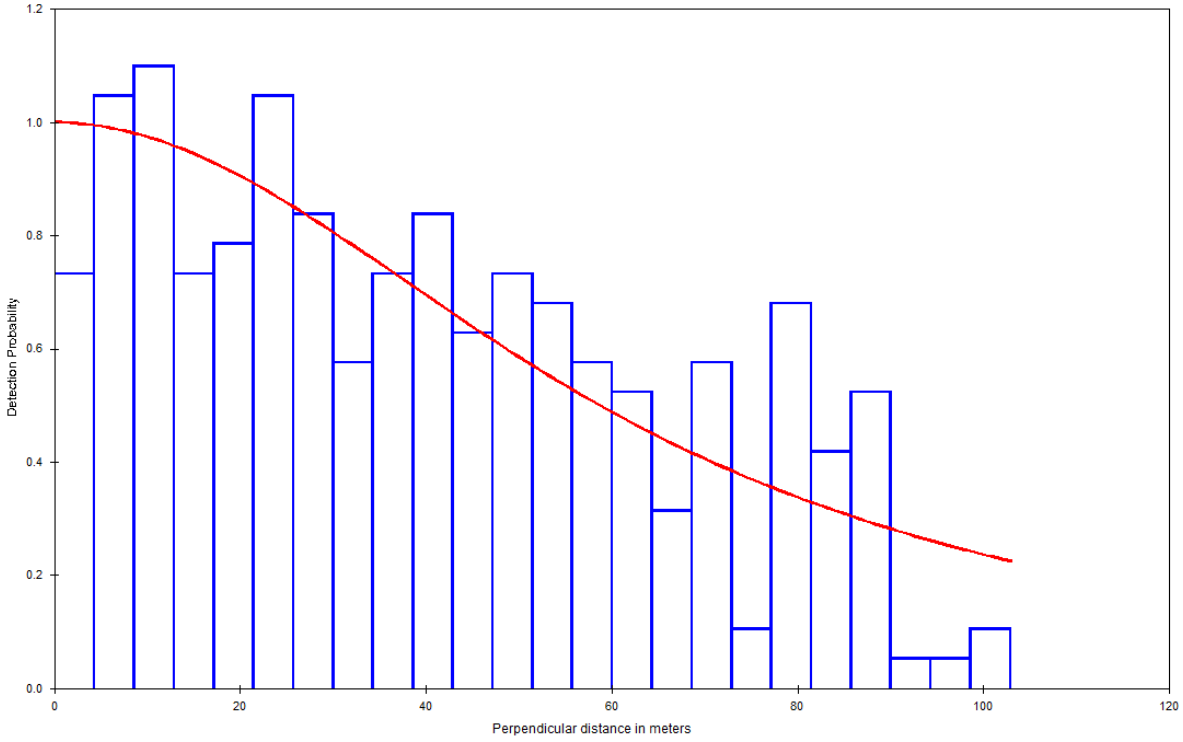

Figure 2: *Decay in the probability of detecting adult horses with increasing distance from the aircraft*

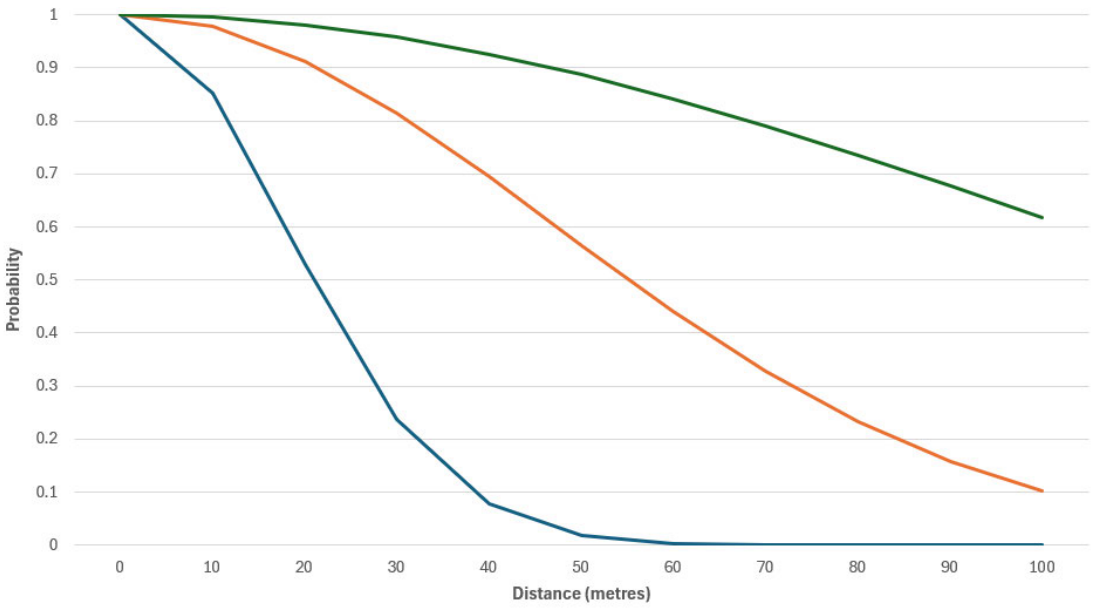

Figure 3: *Decay in the probability of detecting adult horses with increasing distance from the aircraft under three temperature scenarios (blue = 5^{o} C; orange = 15^{o} C; green = 23^{o} C).*

Horses and foals

A range of models were then tested for horses and foals combined (Table 2). As for adult horses, the models tested for the effects of habitat density (open, medium or dense), sun direction, camera position (left, right), the closest time (in decimal hours) to either first light or last light, temperature and humidity.

The best-performing MCDS model with the lowest AIC score (in bold in Table 2) showed that temperature and camera position (left or right) had the greatest effect on combined adult and foal counts. This model had an ESW of 61.2 m and produced a population density estimate of 1.116 horses and foals per km^2 (Table 2).

Table 2: *Multiple covariate distance sampling (MCDS) models tested for adult + foal horse density estimates in three survey blocks of Kosciuszko National Park, 2024 (Cabramurra block was excluded due to insufficient data). The most parsimonious models (lowest AIC score) is shown in bold.*
Abbreviations: *AIC – Akaike's Information Criterion; ESW – effective strip width; LCL – lower confidence limit; UCL – upper confidence limit; CV – coefficient of variation; All models are a half-normal model.*

Model	Delta AIC	AIC	ESW	Density	D LCL	D UCL	D CV
Temp + Camera (F_H)	**0.0**	**2541.4**	**61.2**	**1.116**	**0.770**	**1.617**	**19%**
Temp (F_H)	0.3	2541.7	61.3	1.113	0.769	1.612	19%
Temp + Sun (F_H)	0.5	2542.0	61.1	1.117	0.771	1.619	19%
Temp + Sun + Camera (F_H)	1.0	2542.4	60.9	1.121	0.774	1.625	19%
Temp + Humidity (F_H)	2.1	2543.5	61.2	1.115	0.770	1.615	19%
Temp + Humidity + Cloud (F_H)	2.1	2543.6	61.0	1.120	0.773	1.622	19%
Temp + Habitat (F_H)	2.2	2543.7	61.3	1.114	0.769	1.613	19%
Temp + Humidity + Sun (F_H)	2.3	2543.7	60.9	1.121	0.774	1.625	19%
Temp + Humidity + Habitat (F_H)	4.0	2545.5	61.2	1.116	0.771	1.617	19%
Habitat (Foals and Horses)	14.2	2555.7	62.8	1.087	0.752	1.573	19%
Humidity + Habitat (F_H)	14.7	2556.1	62.6	1.090	0.754	1.577	19%
Habitat + Humidity + Sun (F_H)	15.2	2556.6	62.4	1.093	0.755	1.582	19%
Habitat + Sun (F_H)	15.4	2556.9	62.7	1.089	0.753	1.575	19%
Habitat + HTD (F_H)	16.2	2557.7	62.8	1.087	0.752	1.573	19%
Habitat + Sun + HTD (F_H)	17.4	2558.8	62.7	1.088	0.752	1.574	19%
Humidity (F_H)	22.8	2564.3	64.5	1.059	0.732	1.531	19%
NIL covariates (F_H)	27.3	2568.7	65.1	1.048	0.719	1.527	19%
Sun (F_H)	29.1	2570.6	65.1	1.048	0.725	1.515	19%
Cloud + Sun (F_H)	29.4	2570.8	65.1	1.049	0.726	1.517	19%

Stratified population density & abundance estimates

The best performing models from Table 1 (adult horses) and Table 2 (horses + foals) were then post-stratified over the three included survey blocks, to derive density and abundance

estimates for each block individually (Table 3). The detection function *g(x)* used in the stratified calculations was determined globally for all blocks. The density and abundance estimates in Table 3 are presented with 95% confidence intervals because these were specifically requested; however, we consider the coefficient of variation and standard errors to be more valid indicators of statistical variability in this context (see [redacted] 2024a), and the survey effort was decided based on expected CVs ([redacted], 2024b).

Including foals in addition to adult horses resulted in slightly elevated densities in all three blocks (Table 3). Calculated abundances were fairly similar between the Northern and Southern blocks (Northern Block: 1,369 adult horses or 1,393 horses + foals; Southern Block: 1,226 adult horses or 1,420 horses + foals). The Snowy Plains, which is about an order of magnitude smaller than the other blocks, had an estimated population size of 151–164 horses, but with very high coefficients of variation (66% for adult horses; 68% for adult horses plus foals), which is expected with a smaller area, having a much smaller survey effort.

Table 3: *Estimated horse population density & abundance from thermal camera data, using the best model for adult horses from Table 1, and the best model for adult horses + foals from Table 2, stratified into each survey block. CV = coefficient of variation. LCL and UCL refer to the lower and upper 95% confidence intervals of the abundance.*

		Adult Horses					**Horses and Foals**				
Survey Block	Area (km^2)	Density (horses per km^2)	CV	Abundance	LCL	UCL	Density (horses per km^2)	CV	Abundance	LCL	UCL
Northern	1,229.1	1.114	30%	**1,369**	763	2440	1.134	30%	**1,393**	777	2497
Southern	1,145.7	1.071	26%	**1,226**	742	2011	1.239	25%	**1,420**	791	2095
Snowy Plains	160.9	0.939	66%	**151**	45	505	1.018	68%	**164**	47	568
			Total	**2,746**				**Total**	**2,977**		

Comparison of thermal camera & aerial observer population estimates

Figures 4 and 5 compare the horse population estimates derived from the thermal camera data versus data collected by human aerial observers during the same survey flights. The thermal camera population estimates are from Table 3 of this report, and the equivalent MCDS and MRDS estimates obtained from the simultaneous survey by aerial observers are those reported in [redacted] (2024a).

Figure 4 shows the combined estimates for adult horses plus foals, while Figure 5 shows estimates for adult horses alone, without the inclusion of the foal data. Comparing the two figures provides an indication of the relative performance of thermal cameras and aerial observers for detecting foals, which might be expected to differ from adults given that their smaller body size effectively makes them more similar to adults of smaller species such as deer. The error bars in Figures 4 and 5 represent the standard error of the means (SEs) of each abundance estimate.

For the Northern Block (three left-most columns in Figures 4 and 5), the population estimates from the thermal camera survey were lower than those derived from the aerial observer counts, and particularly so compared to the MRDS estimates. The thermal camera estimate was more similar to the aerial observer MCDS estimate when foals were excluded (Figure 5) than when they were included (Figure 4).

Comparative results for the Southern Block (three central columns in Figures 4 and 5) differed markedly from those of the Northern Block. When horses and foals were included (Figure 4), the thermal camera population estimate of 1,420 animals very closely approximated that of the aerial observer MRDS estimate (1,461 animals), and was considerably elevated compared to the aerial observer MCDS estimate (1,050 animals). When foals were excluded (Figure 5), the thermal camera estimate for adult horses (1,226) fell below that of the MRDS estimate (1,488), but still produced higher figure than the aerial observer MCDS estimate (987 horses).

Too few data were available from the Snowy Plains survey block to say anything conclusive, but the estimates from thermal cameras were broadly in agreement with the aerial observer counts (see final three columns in Figures 4 and 5).

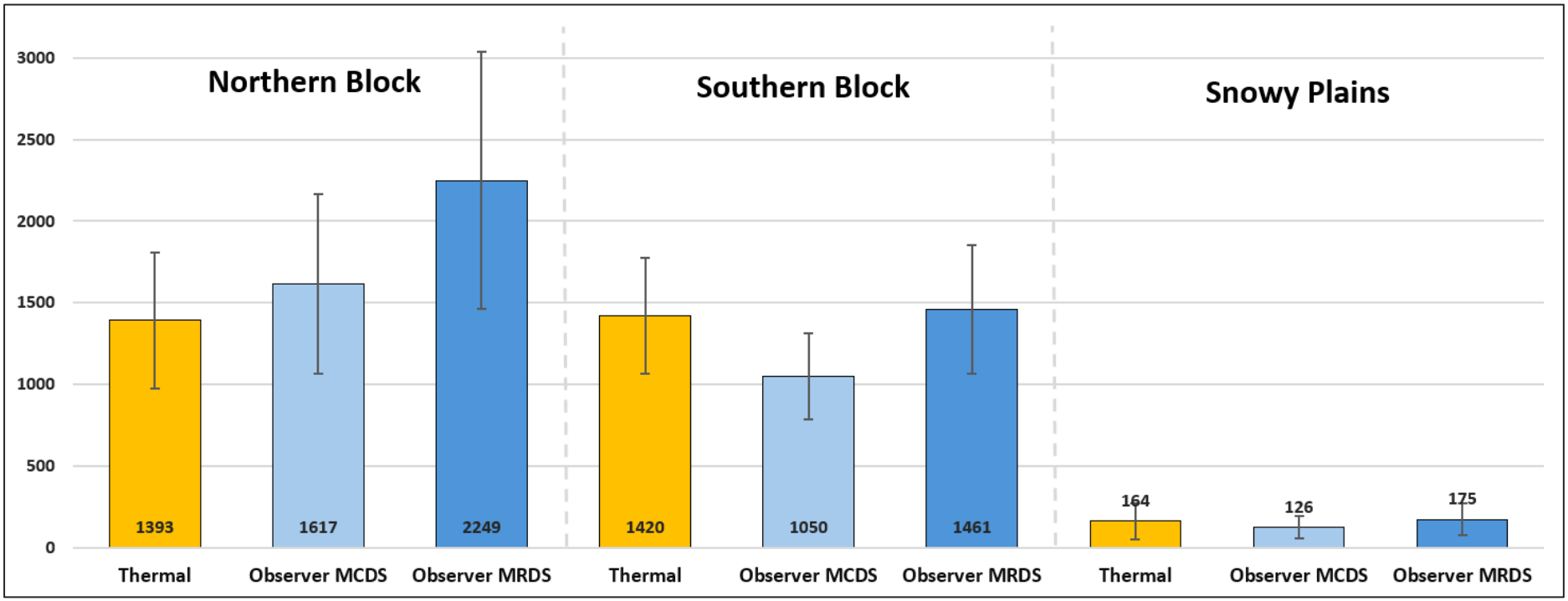

Figure 4: *Comparison of horse+foal population abundance estimates for three survey blocks of Kosciuszko National Park in 2024, calculated from thermal camera (yellow) and aerial observer (blue) data collected simultaneously during the same helicopter flights. Thermal camera estimates are based on data in Table 3 of this report. Aerial observer MCDS and MRDS estimates are from* [redacted] *(2024a).* ***Abbreviations:*** *MCDS – multiple covariate distance sampling; MRDS – mark-recapture distance sampling.* Error bars show the standard error of the means (SEs).

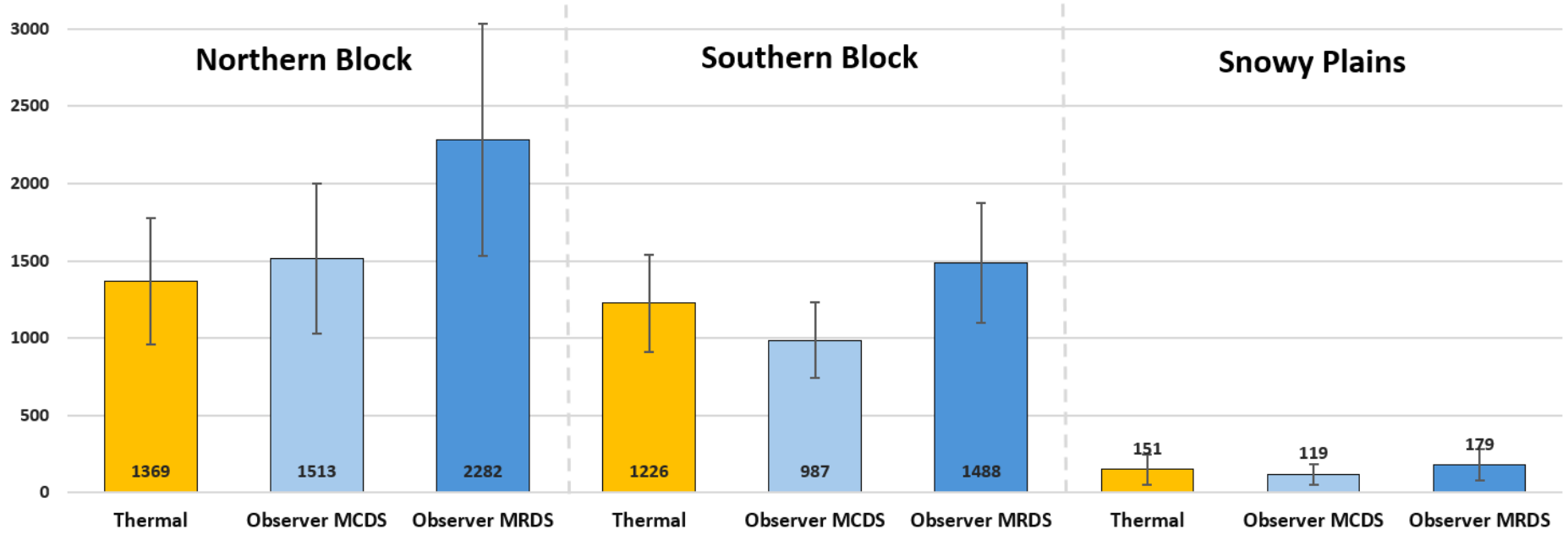

Figure 5: *Comparison of adult horse population abundance estimates for three survey blocks of Kosciuszko National Park in 2024, calculated from thermal camera (yellow) and aerial observer (blue) data collected simultaneously during the same helicopter flights. Thermal camera estimates are based on data in Table 3 of this report. Aerial observer MCDS and MRDS estimates are from* [redacted] *(2024a).* ***Abbreviations:*** *MCDS – multiple covariate distance sampling; MRDS – mark-recapture distance sampling. Error bars show the standard error of the means (SEs).*

Discussion and Summary

Key findings

In the absence of knowing the true population, we can never be definite about which of the approaches (observers or thermal) is closer to the true population. This means the following comparisons are relative comparisons and do not imply any one technique is better than the other.

In the Snowy Plains, which is much smaller than the other included survey blocks, little difference was evident between survey methods.

Relative performance of the thermal cameras and aerial observers differed between the other two survey blocks. Notably, in the Northern Block, both the human aerial observer estimates (MCDS and MRDS) gave considerably higher estimates the thermal cameras. This was the case regardless of whether hoses and foals (Figure 4) or only adult horses (Figure 5) were included. By contrast, in the Southern Block the thermal camera estimates were higher than the aerial observer MCDS estimates, both for horses and foals and for adult horses only, and when foals were included, the thermal camera estimate closely approached the aerial observer MRDS estimate (Figure 4). While this cannot be tested with an ANOVA, the MRDS estimates versus the thermal estimates are most likely not significantly different in the Southern Block, with both abundances falling inside of the error bars of the other.

Overall, the thermal camera estimates are lower than the MRDS estimates in all blocks. Interestingly, they are not always lower than the MCDS estimates. One issue we suspect might be at play was the angle of the cameras (perpendicular to the aircraft track) relative to the human observers who as a rule, look slightly forward of the aircraft to pick up animals before they potentially flush under the aircraft or out of sighting zone 5 (>150 metres out). Thus on some occasions the cameras might have missed horses which the observers saw.

Conversely, it maybe that *p(0)* in the mark-recapture component of aerial observation analysis, differs in each block. There was insufficient data to be able to calculate a different *p(0)* in each survey block.

We investigated the flushing effect further by randomly sampling 130 groups of horses seen by aerial observers in easily identifiable and isolated groups spaced more than 500 m apart. Of these 130 groups, 80 (61.5%) had horses sighted in sighting zones 4 and 5. Of these 80 groups, exactly 50% (40 groups) had no horses seen in the cameras in the near vicinity of the observer sightings. This suggests that some of the horses that aerial observers saw had already been flushed away from the aircraft and out of view of the cameras.

One could theoretically combat this problem by aiming the cameras forward of the aircraft. However, aiming them forward creates a new problem, where the probability of identifying an animal in the thermal footage is then not equal across the frame. This is because the camera's frame would now become an augmented trapezoidal shape on the ground with the (see Figure 6). This is not an issue for distance sampling when the frame is perpendicular to the aircraft track. However, if the cameras face forward by more than say 15°, the probability of sighting an animal begins to become heteroscedastic and not diminishing

gracefully with distance out from the camera, an important assumption in Distance Sampling (Lethbridge et al. 2020). This is illustrated in Figure 6, where the probability of identifying Animal B correctly is much lower than the probability of identifying Animal A, because at 60 frames per second Animal A is available in view for many more video frames than Animal B. The reason this is important is that it often takes several frames to make a positive identification, particularly if the animal's shape is momentarily obscured. The movement patterns of different species also vary, so movement can also improve their identification.

Because Animal B in Figure 6 is closer to the aircraft, distance sampling methodology assumes this has a higher probability of being both seen and correctly identified than Animal A. This means that the forward-angled camera scenario in Figure 6 would violate the assumptions of distance sampling, and other mathematical methods may or may not be valid in explicitly dealing with this phenomenon. This needs further investigation.

If mathematically this cannot be dealt with, and animal flushing is the prevailing reason for the lower camera count compared to the human observer count, we would recommend helicopter platforms are unsuitable for thermography for horses, if they are flushing readily due their wariness of helicopters.

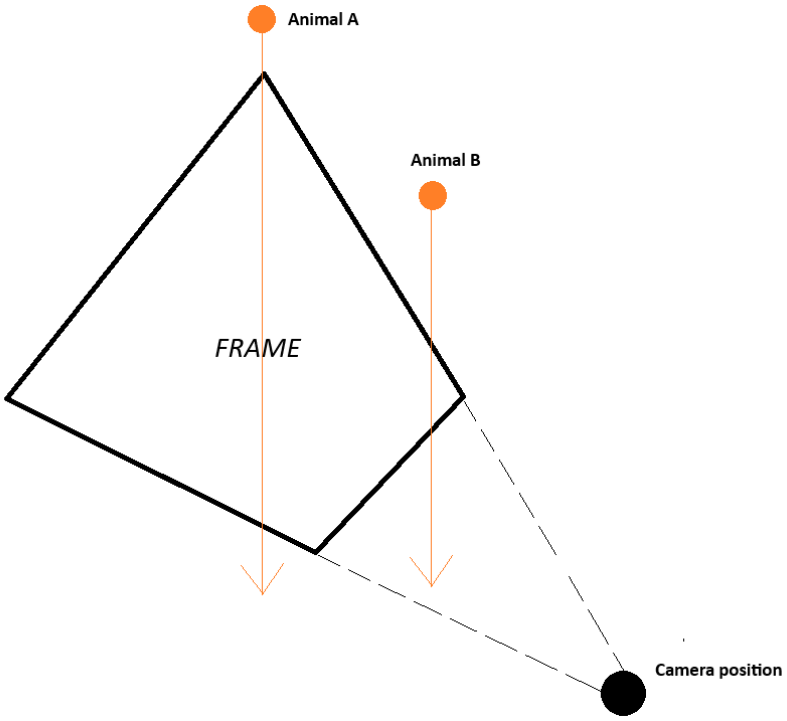

Figure 6: *A hypothetical scenario of pointing the camera forward of the aircraft. Here the probability of identifying Animal B is much lower than Animal A because it is viewed for a smaller period in the camera footage.*

Limitations

Flying the two methods (thermal camera and aerial observers) simultaneously allowed a direct comparison to be made between results, albeit noting the different ESWs (61–62 m for the thermal cameras; ~113–114 m for aerial observers depending on which model was used, see [redacted], 2024a). However, one major limitation of the comparisons is that both methods would be subject to similar biases resulting from any common factors affecting the flight. In other words, they are not completely independent methods. Biases affecting both could have resulted from horse behaviour or common environment and flight conditions. For example, results of the aerial observer survey ([redacted] 2024a) were unclear on whether the lower-than-expected horse numbers in 2024 after culling, may have been the result of emigration, horse flushing behaviour, or horses evading the sound of the helicopter. That report suggested a need to better understand horse movement, as well as how horses respond to low-flying helicopters.

This issue also affects the utility of using thermal cameras in a helicopter. As outlined above (see Figure 6 and associated discussion), if horses flush away from a helicopter and out of the field of view of the thermal cameras, and mathematically there is no 'fix' for violations of the assumptions of distance sampling, we suggest that helicopter platforms are unsuitable for thermography for horses, particularly if they are flushing readily due their wariness of helicopters.

As an alternative to a helicopter, one could attempt flying a UAV Beyond Visual Line of Sight (BVLoS) at night, using the same HD resolution thermal camera technology (i.e. Vayu 1,200 x 1,900 pixel resolution). Approximately 60% of commercial UAV operators in rural areas have reported eagle attacks or near-attacks at some point in their work during day operations. BVLoS operations increase this risk. So night operations are much safer for this technology. If this were an electric drone (thus much quieter than combustion engine drones) there would also be less risk of flushing and/or evasion behaviour by horses. However, night operation would need to be carefully planned so that horses were not roosting at the time of the survey in thicker canopies.

Fixed wing crewed aircraft (usually travelling above 95 knots) are too fast for thermal camera detections, which is why drones and crewed helicopters are the most desirable platforms.

We maintain that video and still aerial photography is not suitable, particularly under canopies. However, other new technologies are emerging that could do away completely with aerial observers and possibly thermal technology in low-flying aircraft. We suggest the NSW government keeps abreast of new technologies so that they can assess their merit in this type of work.

References

Akaike H. 1974 'A new look at the statistical model identification' *IEEE Transactions on Automatic Control* 19 (6): 716–723.

Buckland S. T. Anderson D. R. Burnham K. P. & Laake J. L. (1993). *Distance Sampling: Estimating Abundance of Biological Populations* Chapman and Hall London.

[redacted] (2020). The results of a survey of the wild horse populations in the Kosciuszko National Park, October-November 2020. Report to the NSW Department of Planning, Industry and Environment.

[redacted] (2022). A survey of the wild horse population in the Kosciuszko National Park, November 2022. A report to the NSW National Parks and Wildlife Service.

[redacted] (2023). A survey of the wild horse population in Kosciuszko National Park, October 2023. A report to the NSW National Parks and Wildlife Service. Environment and Heritage Group (2021; amended 2023).

Environment & Heritage Group (2021; amended 2023). Kosciuszko National Park Wild Horse Heritage Management Plan, NSW National Parks & Wildlife Service, Department of Planning & Environment, NSW.

Thomas L. S.T. Buckland E.A. Rexstad J. L. Laake S. Strindberg S. L. Hedley J. R.B. Bishop T. A. Marques and K. P. Burnham (2010). Distance software: design and analysis of distance sampling surveys for estimating population size. *Journal of Applied Ecology* 47: 5–14.

Lethbridge, M.R. (2018). Program *RGIS*.

Lethbridge M (2019). Program *Thermal*.

Lethbridge M (2022). Program *FrameLinkMulti, Version 1.0.*

[redacted] (2024a). A survey of the wild horse population in Kosciuszko National Park, NSW, October–November 2024. *Report to the NSW Department of Climate Change, Energy, the Environment & Water.*

[redacted] (2024b). Review of aerial survey data & methods for estimating wild horse (*Equus caballus*) population density in Kosciuszko National Park, with operational recommendations for the 2024 survey. Report to the NSW Department of Climate Change, Energy, the Environment & Water.